Eur. Phys. J. B (2012) 85: 371
DOI: 10.1140/epjb/e2012-30286-8

THE EUROPEAN PHYSICAL JOURNAL B

Regular Article

Exponential decay of Laplacian eigenfunctions in domains with branches of variable cross-sectional profiles

A.L. Delitsyn[1], B.T. Nguyen[2], and D.S. Grebenkov[2,3,4,a]

[1] Mathematical Department of the Faculty of Physics, Moscow State University, 119991 Moscow, Russia
[2] Laboratoire de Physique de la Matière Condensée (UMR 7643), CNRS – École Polytechnique, 91128 Palaiseau, France
[3] Laboratoire Poncelet (UMI 2615), CNRS – Independent University of Moscow, Bolshoy Vlasyevskiy Pereulok 11, 119002 Moscow, Russia
[4] Chebyshev Laboratory, Saint Petersburg State University, 14th line of Vasil'evskiy Ostrov 29, Saint Petersburg, Russia

Received 3 April 2012 / Received in final form 10 September 2012
Published online 14 November 2012 – © EDP Sciences, Società Italiana di Fisica, Springer-Verlag 2012

Abstract. We study the behavior of the Laplace operator eigenfunctions in an arbitrary resonator (or waveguide) with branches of variable cross-sectional profiles. When an eigenvalue is below a threshold which is determined by the shape of the branch, the associated eigenfunction is proved to have an upper bound which exponentially decays inside the branch. The decay rate is shown to be twice the square root of the difference between the threshold and the eigenvalue. A finite-element numerical solution of the eigenvalue problem illustrates and further extends the above theoretical result which may help to design elaborate resonators or waveguides in microelectronics, optics and acoustics.

1 Introduction

The Laplace operator eigenfunctions play a crucial role in different fields of physics: vibration modes of a thin membrane, standing waves in optical or acoustical cavity resonators, the natural spectral decomposition basis for diffusive processes, the eigenstates of a single trapped particle in quantum mechanics, etc. For the unit interval, the spectrum of the Laplace operator is particularly simple, and the eigenfunctions are just linear combinations of Fourier harmonics $\{e^{i\pi nx}\}$. The oscillating character of eigenfunctions is then often expected for domains in two and higher dimensions. The "scholar" examples of the explicit eigenbases in rectangular and circular domains strongly support this oversimplified but common view. At the same time, the geometrical structure of eigenfunctions may be extremely complicated even for simple domains (e.g., the structure of nodal lines of degenerate eigenfunctions in a square [1]). The more complex the domain is, the more sophisticated and sometimes unexpected the behavior of the associated eigenfunctions may be. For instance, numerous numerical and experimental studies of the eigenvalue problem in irregular or (pre)fractal domains revealed the existence of weakly localized eigenfunctions which have pronounced amplitudes only on a small subregion of the domain and rapidly decay outside this region [2–14].

In this paper, we investigate the behavior of Laplacian eigenfunctions in domains with branches (Fig. 1). We show

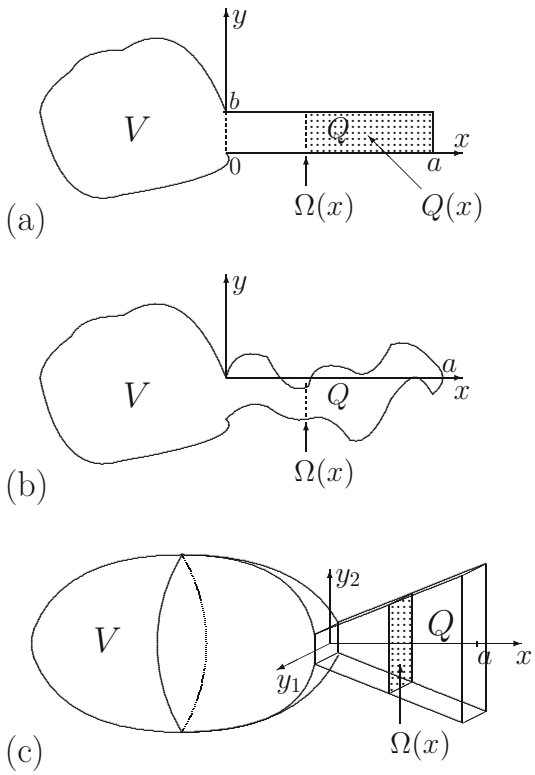

Fig. 1. A bounded domain D is the union of a basic domain V of arbitrary shape and a branch Q with a variable cross-sectional profile $\Omega(x)$.

[a] e-mail: denis.grebenkov@polytechnique.edu

that certain eigenfunctions are "expelled" from the branch, i.e. their amplitude along the branch decays exponentially fast. This kind of "expulsion" effect is well known in optics and acoustics: a wave of wavelength ℓ cannot freely propagate inside a rectangular channel of width b smaller than $\ell/2$ because of the exponential attenuation $\sim e^{-x\pi/b}$ along the channel [15]. We extend this classical result to domains with branches of variable cross-sectional profiles in any dimension. We derive an exponentially decaying upper bound for the L_2-norm of the eigenfunction in cross-sections of the branch, with the sharp decay rate which generalizes and refines the classical rate π/b. Although we focus on bounded domains, the result is also applicable, under certain restrictions, to infinite branches for which this problem is related to localization of waves in optical, acoustical or quantum waveguides (e.g., infinite bent tubes [15–17]). It is worth noting that the exponential decay of eigenfunctions of Schrödinger operators in free space has been thoroughly investigated in physical and mathematical literature (see, e.g., [18–22]).

The paper is organized as follows. In Section 2, we start by considering a two-dimensional domain with a rectangular branch. In this special case, the upper bounds are derived in an elementary way that helps to illustrate the properties of eigenfunctions. Section 3 presents the analysis for domains with branches of variable cross-sectional profiles in any spatial dimension. We provide a sufficient condition on the eigenvalue, under which the related eigenfunction decays exponentially inside the branch. Section 4 presents numerical examples which illustrate the theoretical results and suggest new perspectives for further investigations. The paper ends by conclusions, in which the main results are summarized and their consequences are discussed.

2 Rectangular branch

We begin with the following example (Fig. 1a). We consider the Dirichlet eigenvalue problem

$$-\Delta u = \lambda u, \quad (x,y) \in D, \qquad u|_{\partial D} = 0 \tag{1}$$

in a planar bounded domain $\overline{D} = \overline{V} \cup \overline{Q}$ which is decomposed into a basic domain V of arbitrary shape and a rectangular branch Q of sides a and b: $Q = \{(x,y) \in \mathbb{R}^2: \ 0 < x < a, \ 0 < y < b\}$. We assume that the eigenvalue λ is smaller than the first eigenvalue of the Laplace operator in the cross-section of the branch (i.e., the interval $[0,b]$):

$$\lambda < \pi^2/b^2. \tag{2}$$

Under this condition, we aim to show the exponential decay of the associated eigenfunction u in the branch Q.

In this illustrative example, the derivation is standard and based on an explicit representation of the eigenfunction u. In fact, one can easily check that a general solution of equation (1) in the rectangular branch Q has a form

$$u(x,y) = \sum_{n=1}^{\infty} c_n \sinh(\gamma_n(a-x)) \sin(\pi n y/b), \tag{3}$$

where $\gamma_n = \sqrt{(\frac{\pi}{b}n)^2 - \lambda}$, and c_n are constants. In order to quantify the decay of an eigenfunction u along the branch, we consider the energetic norm of u in the subdomain $Q(x_0) = \{(x,y) \in \mathbb{R}^2: \ x_0 < x < a, \ 0 < y < b\}$ which is defined as

$$||\nabla u||^2_{L_2(Q(x_0))} \equiv \int\limits_{Q(x_0)} (\nabla u, \nabla u) dxdy. \tag{4}$$

Substituting equation (3) to (4) yields

$$||\nabla u||^2_{L_2(Q(x_0))} = \sum_{n=1}^{\infty} c_n^2 \frac{b}{2} \int\limits_{x_0}^{a} \Big[\Big(\frac{\pi}{b}n\Big)^2 \sinh^2(\gamma_n(a-x)) + \gamma_n^2 \cosh^2(\gamma_n(a-x)) \Big] dx. \tag{5}$$

Using elementary inequalities for the integral (see Appendix A), one gets

$$||\nabla u||^2_{L_2(Q(x_0))} \le C e^{-2\gamma_1 x_0} \sum_{n=1}^{\infty} n c_n^2 \sinh^2(\gamma_n a), \tag{6}$$

where C is an explicit constant. The trace theorem provides the upper bound for the above series (Appendix A)

$$||\nabla u||^2_{L_2(Q(x_0))} \le C_1 ||u||^2_{L_2(D)} e^{-2\gamma_1 x_0},$$

with another explicit constant C_1. Note that $||u||^2_{L_2(D)}$ is a constant which is often set to 1 as a normalization of eigenfunctions. So, we established the exponential decay of the energy $||\nabla u||^2$ in the branch Q with the decay rate $2\gamma_1 = 2\sqrt{(\frac{\pi}{b})^2 - \lambda}$, under the sufficient condition (2). In other words, the energy $||\nabla u||^2_{L_2(Q(x_0))}$ stored at the branch end $Q(x_0)$ decays exponentially fast when the distance x_0 to the basic domain V increases. The derivation implies that the decay rate of the upper bound is sharp (i.e., it cannot be improved in general).

The above inequality implies a similar upper bound for the L_2-norm which is weaker than the energetic norm (4). In fact, one has

$$||u||^2_{L_2(Q(x_0))} \equiv \int\limits_{Q(x_0)} u^2 dxdy = \int\limits_{x_0}^{a} dx \ (u,u)_{L_2(\Omega(x))} \le \int\limits_{x_0}^{a} dx \frac{1}{\mu} (\nabla u, \nabla u)_{L_2(\Omega(x))} = \frac{1}{\mu} ||\nabla u||^2_{L_2(Q(x_0))},$$

from which one gets

$$||u||^2_{L_2(Q(x_0))} \le C_2 ||u||^2_{L_2(D)} e^{-2\gamma_1 x_0}, \tag{7}$$

where C_2 is another constant, $\mu = (\pi/b)^2$ is the first eigenvalue in the cross-section $\Omega(x) = [0,b]$ of the branch Q, and the intermediate inequality followed from the Rayleigh quotient for the cross-section

(see Appendix B.1). The L_2-norm is another quantitative measure for smallness of an eigenfunction in a subregion $Q(x_0)$ of the domain.

It is worth noting that no information about the basic domain V was used. In particular, the Dirichlet boundary condition on ∂V can be replaced by arbitrary boundary condition under which the Laplace operator is still self-adjoint.

3 Branch of arbitrary shape

Using a general method of differential inequalities, we now show that the above upper bound remains valid for eigenfunctions in a much more general case with a branch of arbitrary shape in $\mathbb{R}^{n+1}$ $(n = 1, 2, 3, \ldots)$. In contrast to Section 2, this method does not require an explicit representation of eigenfunctions that allows, for the first time, to deal with branches of variable cross-sectional profiles.

We consider the eigenvalue problem

$$-\Delta u(x,\mathbf{y}) = \lambda u(x,\mathbf{y}), \quad (x,\mathbf{y}) \in D, \qquad u|_{\partial D} = 0, \quad (8)$$

where $\overline{D} = \overline{V} \cup \overline{Q}$ is decomposed into a basic bounded domain $V \subset \mathbb{R}^{n+1}$ of arbitrary shape and a branch $Q \subset \mathbb{R}^{n+1}$ of a variable cross-sectional profile $\Omega(x) \subset \mathbb{R}^n$ (Figs. 1b, 1c):

$$Q = \{(x,\mathbf{y}) \in \mathbb{R}^{n+1}\colon\ \mathbf{y} \in \Omega(x),\ 0 < x < a\}.$$

Each cross-section $\Omega(x)$ is a bounded domain which is parameterized by x from 0 to a. The branch Q is assumed to be simply-connected, while its boundary is smooth. Although weaker conditions on the shape of the branch can be used (see discussion in Sect. 4.1), their justification would require a substantial technical analysis which is beyond the scope of the paper [23].

For a fixed x, let $\mu_1(x)$ be the first eigenvalue of the Dirichlet eigenvalue problem in the cross-section $\Omega(x)$

$$-\Delta_\perp \phi(\mathbf{y}) = \mu_1(x)\phi(\mathbf{y}), \quad \mathbf{y} \in \Omega(x), \qquad \phi|_{\partial\Omega(x)} = 0, \quad (9)$$

where $\Delta_\perp$ is the n-dimensional Laplace operator. We denote

$$\mu = \inf_{0<x<a} \mu_1(x) \quad (10)$$

the smallest first eigenvalue among all cross-sections of the branch. For example, for a rectangular branch with $\Omega(x) = [0, b]$ (independent of x), one has $\mu = \pi^2/b^2$ and retrieves the example from Section 2.

Now, we can formulate the main result of the paper. If the basic domain V is large enough so that

$$\lambda < \mu, \quad (11)$$

we prove that the squared L_2-norm of the eigenfunction u in the cross-section $\Omega(x_0)$,

$$I(x_0) \equiv \int\limits_{\Omega(x_0)} u^2(x_0,\mathbf{y})d\mathbf{y}, \quad (12)$$

has an upper bound which decays exponentially with x_0:

$$I(x_0) \le I(0)e^{-\beta x_0} \quad (0 \le x_0 < a), \quad (13)$$

with the decay rate

$$\beta = \sqrt{2}\,\sqrt{\mu - \lambda}. \quad (14)$$

Moreover, if the branch profile $\Omega(x)$ satisfies the condition

$$(\mathbf{e}_x, \mathbf{n}(x,\mathbf{y})) \ge 0 \quad \text{for almost all } (x,\mathbf{y}) \in \partial Q, \quad (15)$$

where $\mathbf{e}_x$ is the unit vector along the x coordinate, and $\mathbf{n}(x,\mathbf{y})$ the unit normal vector at the boundary point $(x,\mathbf{y})$ directed outwards the domain, then the decay rate is improved:

$$\beta = 2\sqrt{\mu - \lambda}. \quad (16)$$

Qualitatively, the condition (15) means that the branch Q is not increasing. Note that the example of a rectangular branch from Section 2 shows that the decay rate in equation (16) is sharp (cannot be improved in general). We first prove the inequality (13) and then discuss its implications and provide numerical illustrations in Section 4. Although the proof is instructive, a less experienced reader may skip it and move directly to Section 4.

The proof consists in three steps.

(i) First, we derive the inequality

$$I''(x_0) \ge c\gamma^2 I(x_0), \quad (17)$$

where $c = 2$ for arbitrary branch and $c = 4$ for branches satisfying the condition (15), and $\gamma = \sqrt{\mu - \lambda}$. This type of inequalities was first established by Maslov for Schrödinger operators in free space [21,22]. For this purpose, we consider the first two derivatives of $I(x_0)$:

$$I'(x_0) = 2\int\limits_{\Omega(x_0)} u\frac{\partial u}{\partial x}\,d\mathbf{y}, \quad (18)$$

$$I''(x_0) = 2\int\limits_{\Omega(x_0)} u\frac{\partial^2 u}{\partial x^2}\,d\mathbf{y} + 2\int\limits_{\Omega(x_0)} \left(\frac{\partial u}{\partial x}\right)^2 d\mathbf{y}, \quad (19)$$

where the boundary condition $u|_{\partial Q} = 0$ cancels the integrals over the "lateral" boundary of $Q(x_0)$.

The first integral in equation (19) can be bounded as

$$\begin{aligned}\int\limits_{\Omega(x_0)} u\frac{\partial^2 u}{\partial x^2}d\mathbf{y} &= \int\limits_{\Omega(x_0)} u\big[\Delta u - \Delta_\perp u\big]\,d\mathbf{y} \\ &= \int\limits_{\Omega(x_0)} (\nabla_\perp u, \nabla_\perp u)d\mathbf{x} \\ &\quad - \lambda\int\limits_{\Omega(x_0)} u^2 d\mathbf{y} \ge (\mu - \lambda)\int\limits_{\Omega(x_0)} u^2 d\mathbf{y},\end{aligned} \quad (20)$$

where we used the Friedrichs-Poincaré inequality for the cross-section $\Omega(x_0)$ (see Appendix B.1):

$$\int\limits_{\Omega(x_0)} (\nabla_\perp u, \nabla_\perp u) d\mathbf{y} \geq \mu_1(x_0) \int\limits_{\Omega(x_0)} u^2 d\mathbf{y} \geq \mu \int\limits_{\Omega(x_0)} u^2 d\mathbf{y}, \tag{21}$$

and $\mu_1(x_0) \geq \mu$ by definition of μ in equation (10). Since the second term in equation (19) is always positive, one has

$$I''(x_0) \geq 2 \int\limits_{\Omega(x_0)} u \frac{\partial^2 u}{\partial x^2} d\mathbf{y} \geq 2(\mu - \lambda) \int\limits_{\Omega(x_0)} u^2 d\mathbf{y},$$

from which follows the inequality (17) with $c = 2$.

If the condition (15) is satisfied, a more accurate bound of the second term in equation (19) follows from the Rellich's identity (see Appendix B.2):

$$\int\limits_{\Omega(x_0)} \left(\frac{\partial u}{\partial x}\right)^2 d\mathbf{y} = \int\limits_{\Omega(x_0)} (\nabla_\perp u, \nabla_\perp u) d\mathbf{y} - \lambda \int\limits_{\Omega(x_0)} u^2 d\mathbf{y} + \int\limits_{\partial Q(x_0) \setminus \Omega(x_0)} \left(\frac{\partial u}{\partial n}\right)^2 (\mathbf{e}_x, \mathbf{n}(S)) dS, \tag{22}$$

where $Q(x_0)$ denotes a part of the branch Q delimited by $\Omega(x_0)$:

$$Q(x_0) = \left\{(x, \mathbf{y}) \in \mathbb{R}^{n+1} \colon \mathbf{y} \in \Omega(x),\ x_0 < x < a\right\}. \tag{23}$$

The condition (15) implies the positivity of the last term in equation (22), which can therefore be dropped off in order to get the following bound:

$$\int\limits_{\Omega(x_0)} \left(\frac{\partial u}{\partial x}\right)^2 d\mathbf{y} \geq \int\limits_{\Omega(x_0)} (\nabla_\perp u, \nabla_\perp u) d\mathbf{y} - \lambda \int\limits_{\Omega(x_0)} u^2 d\mathbf{y} \geq (\mu - \lambda) \int\limits_{\Omega(x_0)} u^2 d\mathbf{y}.$$

Combining this result with (20), one gets the inequality (17) with $c = 4$.

(ii) Second, we prove the following relations

$$I(a) = 0, \quad I'(a) = 0, \quad I(x_0) \neq 0, \quad I'(x_0) < 0 \tag{24}$$

for $0 \leq x_0 < a$. In fact, taking into account equation (18) and applying the Green's formula in subdomain $Q(x_0)$, one obtains

$$I'(x_0) = -2 \int\limits_{Q(x_0)} u \Delta u \, dx d\mathbf{y} - 2 \int\limits_{Q(x_0)} (\nabla u, \nabla u) dx d\mathbf{y}, \tag{25}$$

where the boundary condition $u|_{\partial Q(x_0) \setminus \Omega(x_0)} = 0$ canceled boundary integrals. The second term can be bounded by using again the Friedrichs-Poincaré inequality (21):

$$\begin{aligned} \int\limits_{Q(x_0)} (\nabla u, \nabla u) dx d\mathbf{y} &= \int\limits_{Q(x_0)} \left[\left(\frac{\partial u}{\partial x}\right)^2 + (\nabla_\perp u, \nabla_\perp u)\right] dx d\mathbf{y} \\ &\geq \int\limits_{x_0}^{a} dx \int\limits_{\Omega(x)} (\nabla_\perp u, \nabla_\perp u) d\mathbf{y} \\ &\geq \mu \int\limits_{x_0}^{a} dx \int\limits_{\Omega(x)} u^2 dx d\mathbf{y} \\ &= \mu \int\limits_{Q(x_0)} u^2 dx d\mathbf{y}. \end{aligned} \tag{26}$$

The equation $\Delta u = -\lambda u$ yields then

$$\begin{aligned} -I'(x_0) &= -2\lambda \int\limits_{Q(x_0)} u^2 dx d\mathbf{y} + 2 \int\limits_{Q(x_0)} (\nabla u, \nabla u) dx d\mathbf{y} \\ &\geq 2(\mu - \lambda) \int\limits_{Q(x_0)} u^2 dx d\mathbf{y} \geq 0, \end{aligned}$$

so that $I(x_0)$ monotonously decays. We emphasize that there is no request on a monotonous decrease of any kind for the cross-section $\Omega(x)$.

Sending x_0 to a in equation (25), one gets $I'(a) = 0$.

Finally, we show that $I(x_0) \neq 0$ for $0 \leq x_0 < a$. Indeed, if there was x_0 such that $I(x_0) = 0$, then the restriction of u to the subdomain $Q(x_0)$ would be a solution of the eigenvalue problem in $Q(x_0)$:

$$-\Delta u = \lambda u, \quad (x, \mathbf{y}) \in Q(x_0), \qquad u|_{\partial Q(x_0)} = 0.$$

Multiplying this equation by u and integrating over the domain $Q(x_0)$ lead to

$$\lambda \int\limits_{Q(x_0)} u^2 dx d\mathbf{y} = \int\limits_{Q(x_0)} (\nabla u, \nabla u) dx d\mathbf{y}.$$

On the other hand, the Friedrichs-Poincaré inequality (26) yields

$$\int\limits_{Q(x_0)} (\nabla u, \nabla u) dx d\mathbf{y} \geq \mu \int\limits_{Q(x_0)} u^2 dx d\mathbf{y},$$

from which $\lambda \geq \mu$, in contradiction to the condition (11). As a consequence, $I(x_0) \neq 0$ for $0 \leq x_0 < a$.

(iii) Third, we establish the exponential decay (13) following the Maslov's method [21,22]. The multiplication of the inequality (17) by $I'(x_0)$ yields

$$((I')^2)' \leq c\gamma^2 (I^2)'.$$

After integrating from x_0 to a, one gets

$$-(I'(x_0))^2 \leq -c\gamma^2 I^2(x_0),$$

where $I(a) = I'(a) = 0$ from equation (24). Taking in account that $I' < 0$, one deduces

$$-I'(x_0) \geq \sqrt{c}\gamma I(x_0).$$

Dividing by $I(x_0)$ and integrating from 0 to x_0 lead to inequality (13) that completes our proof.

As in Section 2, no information about the basic domain V was used so that the Dirichlet boundary condition on ∂V can be replaced by arbitrary boundary condition under which the Laplace operator in D remains self-adjoint.

4 Discussion

The main result of Section 3 is the inequality (13) which states that if an eigenvalue λ in the whole domain D is below the smallest eigenvalue μ in all cross-sections $\Omega(x)$ of a branch Q, the associated eigenfunction u decays exponentially in the branch Q. The decay is quantified through the L_2-norm of u at cross-sections $\Omega(x_0)$ which is shown to have the upper bound exponentially decreasing with the "distance" x_0 between the cross-section $\Omega(x_0)$ and the basic domain V. It is worth stressing a purely spectral character of the decay rate β which depends on the different between the smallest eigenvalue μ in all cross-sections of the branch and the eigenvalue λ in the whole domain D. Generally speaking, narrower cross-sections imply larger μ and yield thus stronger attenuation of eigenfunctions. This quantifies the idea of "expulsion" of an eigenfunction from narrow regions of a domain.

The condition (11) on the eigenvalue λ in D can be replaced by another condition

$$\kappa < \mu \tag{27}$$

on the eigenvalue κ in the basic domain V:

$$-\Delta\phi = \kappa\phi, \quad (x, \mathbf{y}) \in V, \qquad \phi|_{\partial V} = 0. \tag{28}$$

According to the Rayleigh's principle, the inequality (27) is sufficient for the existence of the eigenvalue λ lying below μ (see Appendix B.1). Although the condition (27) is *stronger* than (11), it may be preferred for studying different branches Q attached to the same domain V (in which case, the eigenvalue κ has to be computed only once).

Looking at the derivation of the inequality (13), many questions naturally appear: how accurate the upper bound is? Is the condition (15) necessary for getting the sharp decay rate according to equation (16)? How do the eigenfunctions with λ larger than μ behave? Is the exponential decay applicable for other boundary conditions? In the next subsection, we address these questions through numerical solutions of the eigenvalue problem in planar domains.

4.1 Two-dimensional branches

In order to answer these and some other questions, we consider several planar bounded domains D which are all composed of the unit square V as the basic domain and a branch Q of different shapes (Fig. 2). The eigenvalue problem (8) in these domains with Dirichlet boundary condition was solved numerically by a finite-element method in Matlab PDEtools. Once the eigenfunctions and eigenvalues are found, we approximate the squared L_2-norm of the eigenfunction u_n in the subregion $Q(x_0) = \{(x, y) \in Q\colon\ x_0 < x < a\}$ of the branch Q as

$$J_n(x_0) \equiv \int\limits_{Q(x_0)} u_n^2(x, y)dxdy \simeq \sum_T \frac{S(T)}{3} \sum_{j=1}^{3} u_n^2\left(x_j^T, y_j^T\right), \tag{29}$$

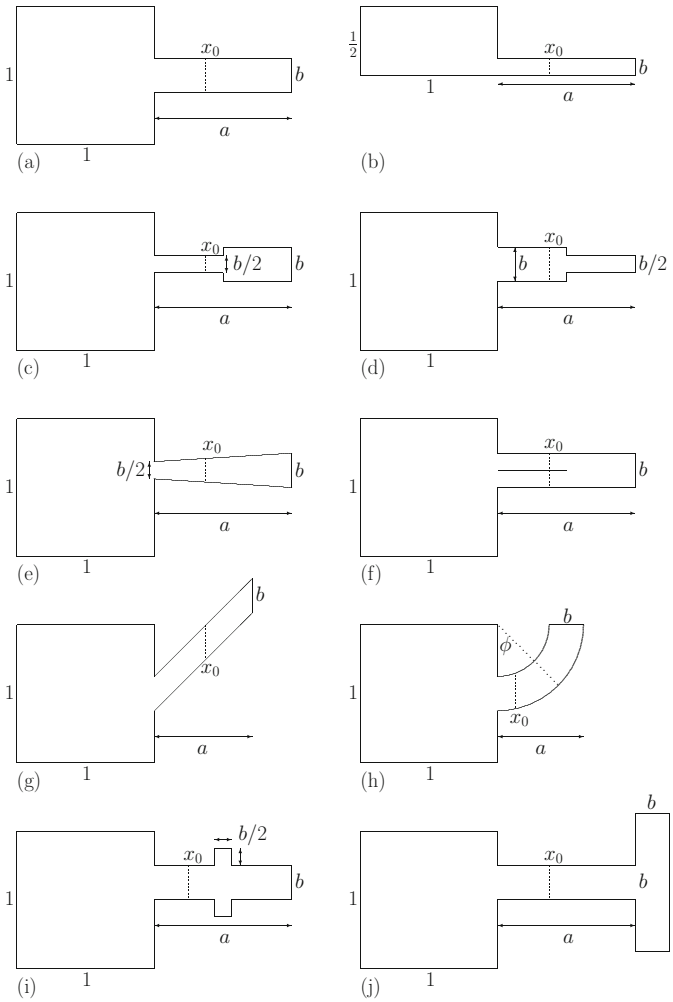

Fig. 2. The unit square (basic domain V) and several shapes of the branch Q: (a) rectangular branch; (b) half of the domain 'a'; (c) narrow-then-wide channel; (d) wide-then-narrow channel; (e) increasing branch with the width linearly changing from $b/2$ to b; (f) branch with a partial cut at the middle; (g) tilted rectangular branch; (h) circular branch; (i) branch with a small broadening in the middle; (j) bifurcating branch. We set $a = 1$ and $b = 1/4$ in all cases, except 'g' and 'h', for which $a = 1/\sqrt{2}$ and $a = 5/8$, respectively. For shapes 'c', 'd', 'e', 'f', 'i' and 'j', the branch is up shifted by 1/8 in order to break the reflection symmetry (for cases 'g' and 'h', there is no shift because the branch itself has no reflection symmetry).

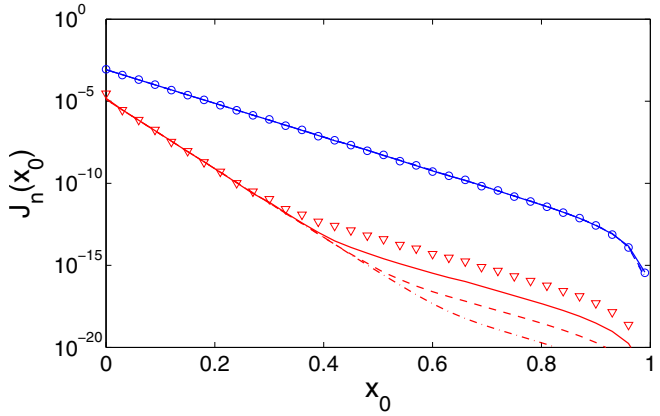

Fig. 3. (Color online) Computation of $J_n(x_0)$ at different levels k of mesh refinement of the rectangular branch in Figure 2a: $k = 3$ (symbols, 6848 triangles in the mesh), $k = 4$ (solid lines, 27 392 triangles), $k = 5$ (dashed lines, 109 568 triangles) and $k = 6$ (dash-dotted lines, 438 272 triangles). For $n = 1$, all these curves fall onto each other, confirming the accurate computation which is independent of the mesh size. In turn, the curves for $n = 3$ coincide only for small x_0 but deviate from each other for larger x_0. The higher k, the closer the curve to the expected exponential decay (see Fig. 4).

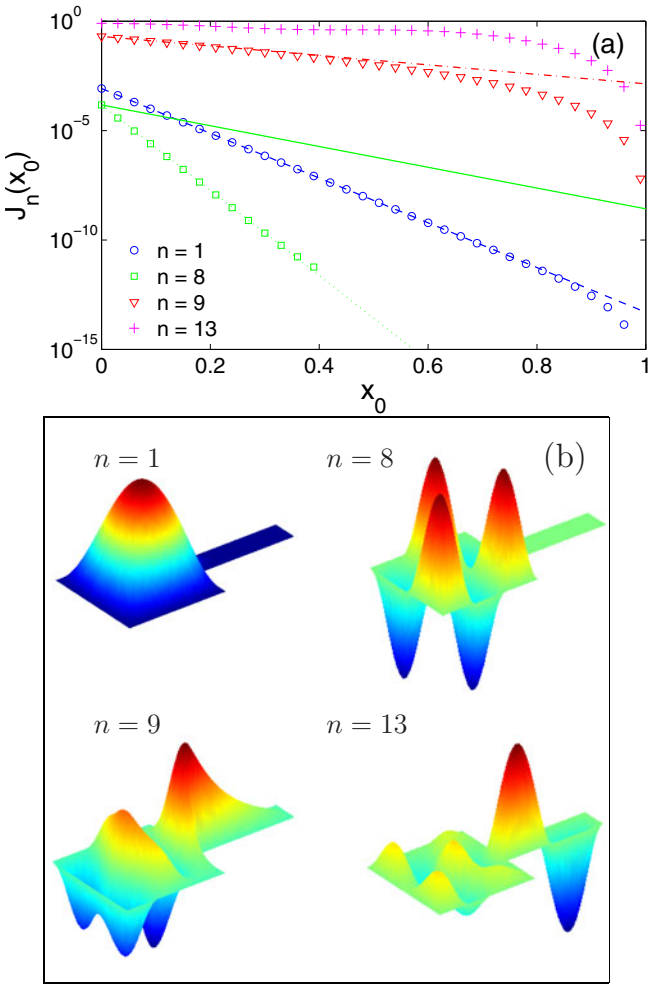

Fig. 4. (Color online) (a) The squared L_2-norm, $J_n(x_0)$, of four eigenfunctions with $n = 1, 8, 9, 13$ (symbols) for the rectangular branch in Figure 2a. The upper bound (31) with $\mu = \pi^2/(1/4)^2$ is plotted by dashed ($n = 1$), solid ($n = 8$) and dash-dotted ($n = 9$) lines. The upper bound (31) with $\mu = \pi^2/(1/8)^2$ is shown for $n = 8$ by dotted line. (b) The corresponding eigenfunctions.

where the sum runs over all triangles T of the mesh, $S(T)$ being the area of the triangle T, and $\{(x_j^T, y_j^T)\}_{j=1,2,3}$ its three vertices. Since the eigenfunctions are analytic inside the domain, the error of the above approximation is mainly determined by the areas of triangles. In order to check whether the results are accurate or not, we computed the function $J_n(x_0)$ at different levels k of mesh refinement (once the initial triangular mesh is generated by Matlab, each level of refinement consists in dividing each triangle of the mesh into four triangles of the same shape). Figure 3 shows the resulting curves for the rectangular branch from Figure 2a. For the first eigenfunction, all the curves fall onto each other, i.e. $J_1(x_0)$ is independent of k, as it should be. In turn, the curves for $n = 3$ coincide only for small x_0 but deviate from each other for larger x_0. The higher k, the closer the curve to the expected exponential decay. This means that even 6 levels of mesh refinement (here, a mesh with 438 272 triangles) is not enough for an accurate computation of the integral $J_3(x_0)$. Among the 20 first eigenfunctions, similar deviations were observed for $n = 3, 4, 8, 10, 14, 15, 17$. The specific behavior of these eigenfunctions seems to be related to their reflection symmetry. Although several improvements could be performed (e.g., higher-order integration schemes instead of Eq. (29)), this is too technical and beyond the scope of the paper because our numerical computations aim only at illustrating the theoretical bounds. After all, the deviations become distinguishable only in the region of x_0 for which $J_n(x_0)$ is negligible (e.g., deviations on Fig. 3 start to appear below 10^{-12}). For all data sets discussed below, we checked the accuracy by performing computations with different k and presented only the reliable data with $k = 5$ (such meshes contain between 100 000 and 170 000 triangles, except for the case in Fig. 2f with 671 744 triangles).

The exponential decay (13) for $I(x_0)$ implies that $J_n(x_0)$:

$$J_n(x_0) = \int_{x_0}^{a} dx\ I_n(x) \le \int_{x_0}^{a} dx\ I_n(0) e^{-2\gamma_n x} \le \frac{I_n(0)}{2\gamma_n} e^{-2\gamma_n x_0}, \tag{30}$$

where

$$\gamma_n = \sqrt{\mu - \lambda_n},$$

and we take $c = 4$ even if the sufficient condition (15) is not satisfied. In what follows, we will check numerically the stronger inequality

$$J_n(x_0) \le J_n(0) e^{-2\gamma_n x_0}, \tag{31}$$

from which (30) follows, because

$$J_n(0) = \int_0^a dx I_n(x) \le I_n(0) \int_0^a dx e^{-2\gamma_n x} \le \frac{I_n(0)}{2\gamma_n}.$$

It is worth stressing that the main inequality (31) for the squared L_2-norm $J_n(x_0)$ in the subregion $Q(x_0)$ is a *weaker* result than the inequality (13) for the squared L_2-norm $I_n(x_0)$ in the cross-section $\Omega(x_0)$. However, the analysis of $I_n(x_0)$ would require an accurate computation of the projection of an eigenfunction u_n, which was computed on a triangular mesh in D, onto the cross-section $\Omega(x_0)$. Since the resulting $I_n(x_0)$ would be less accurate than $J_n(x_0)$, we focus on the latter quantity.

Finally, we outline that for many examples that we consider in this section, the boundary of the branch Q is not smooth (as requested at the beginning of Sect. 3) but piecewise smooth, while its cross-section $\Omega(x)$ is not a continuous function of x. For examples 'c', 'd' , 'i' and 'j' in Figure 2, the expressions for $I'(x)$ and $I''(x)$ are nevertheless well defined because the integrand functions in equations (18) and (19) have no singularities (the behavior of eigenfunctions near angles is well known in the theory of elliptic operators [23]). From a practical point of view, the boundary of these branches can be smoothed at small length scales so that numerical (approximate) solutions for the original and smoothed boundaries would be indistinguishable. In turn, the branch with a partial cut (example 'f') requires more elaborate analysis that goes beyond the scope of the paper. We consider this numerical example in order to illustrate that the conditions for the branch to be simply-connected and for the boundary to be smooth can potentially be relaxed.

Rectangular branch

We start with a rectangular branch of width $b = 1/4$ (Fig. 2a), for which $\mu = \pi^2/(1/4)^2 \simeq 157.91\ldots$, and there are 9 eigenvalues λ_n below μ (the first 20 eigenvalues are listed in Tab. 1). Figure 4a shows $J_n(x_0)$ for four eigenfunctions with $n = 1, 8, 9, 13$. These four eigenfunctions are chosen to illustrate different possibilities. For the eigenmodes with $n = 1, 2, 5, 7, 9$ (illustrated by $n = 1, 9$), the upper bound is very accurate. In this case, the decay rate $2\gamma_n$ is sharp and cannot be improved. There is another group of eigenfunctions with $n = 3, 4, 6, 8$ (illustrated by $n = 8$), for which $J_n(x_0)$ is significantly smaller than the upper bound. For $x_0 < 0.4$, $J_8(x_0)$ decays as $J_8(0)\exp[-2\gamma'_8 x_0]$, where $2\gamma'_8 = 2\sqrt{4\mu - \lambda_8}$ is the improved decay rate (for larger x_0, the computation is inaccurate as explained earlier and its result is not shown). In order to understand this behavior, one can inspect the shape of the eigenfunction $u_8(x, y)$ shown in Figure 4b. This function is anti-symmetric with respect to the horizontal line which splits the domain D into two symmetric subdomains. As a consequence, $u_8(x, y)$ is 0 along this line and it is thus a solution of the Dirichlet eigenvalue problem for each subdomain (Fig. 2b). The width of the branch in each subdomain is twice smaller so that one can apply the general upper bound with $\mu' = 4\mu$. This is a special feature of all symmetric domains.

If the branch was shifted upwards or downwards, the reflection symmetry would be broken, and the decay rate $2\gamma'_n$ would not be applicable any more. However, if the shift is small, one may still expect a faster exponential decrease with the decay rate between $2\gamma_n$ and $2\gamma'_n$. This example shows that the upper bound (13) may not be sharp for certain eigenfunctions. At the same time, it cannot be improved in general, as illustrated by the eigenfunctions with $n = 1, 9$.

The last curve shown in Figure 4a by pluses, corresponds to $n = 13$, for which $\lambda_{13} > \mu$, and the exponentially decaying upper bound (31) is not applicable. One can see that the function $J_{13}(x_0)$ slowly varies along the branch. This behavior is also expected from the shape of the underlying eigenfunction u_{13} shown on Figure 4b.

Table 1. First 20 eigenvalues of the Laplace operator in domains shown in Figure 2.

n	$2a$	$2c$	$2d$	$2e$	$2f$	$2g$	$2h$	$2i$	$2j$
1	19.33	19.66	19.39	19.64	19.58	19.39	19.33	19.39	19.39
2	47.53	48.95	47.58	48.94	48.59	47.86	47.54	47.58	47.58
3	49.32	49.35	49.33	49.35	49.33	49.32	49.32	49.33	49.33
4	78.83	78.75	77.85	78.90	78.54	78.85	78.84	77.85	77.85
5	93.12	97.87	94.41	97.69	97.09	94.48	93.12	94.40	94.41
6	98.70	98.71	98.67	98.71	98.66	98.71	98.71	98.67	98.67
7	126.1	127.8	125.2	127.9	127.3	126.9	126.1	125.2	125.2
8	128.0	128.3	128.0	128.3	128.0	128.1	128.0	128.0	127.7
9	151.7	166.1	154.1	165.8	164.6	158.5	151.6	150.4	128.0
10	167.7	167.8	167.8	167.8	167.8	167.7	167.7	156.8	153.6
11	167.8	177.5	176.5	177.1	177.0	175.8	171.8	167.8	167.8
12	175.3	193.9	182.3	196.9	183.4	196.5	176.1	176.7	167.8
13	191.7	196.1	196.1	197.5	195.3	197.4	196.4	185.3	176.7
14	196.4	197.5	197.4	239.6	197.4	229.6	197.4	197.1	185.4
15	197.4	245.1	229.1	244.4	244.1	245.9	204.5	197.4	195.2
16	218.8	246.8	246.0	246.8	246.2	250.7	235.5	218.5	195.5
17	245.7	254.3	249.2	254.1	252.4	256.7	245.8	242.8	197.4
18	246.7	256.7	256.6	256.7	256.6	284.6	250.5	246.1	214.8
19	252.5	284.7	269.6	285.8	259.3	285.5	256.7	250.6	229.0
20	256.6	286.3	285.9	286.3	283.2	304.1	278.7	256.6	245.9

Narrow/wide and wide/narrow branches

In two dimensions, any cross-section $\Omega(x)$ of a branch Q is a union of intervals. If $\ell(x)$ is the length of the largest interval in $\Omega(x)$ then the first eigenvalue $\mu_1(x)$ in $\Omega(x)$ is simply $\pi^2/\ell(x)^2$. Whatever the shape of the branch is, the threshold μ for the exponential decay is then set by the length of the largest cross-section $b = \max_{0<x<a} \ell(x)$ according to $\mu = \pi^2/b^2$. At first thought, this statement may sound counter-intuitive because one could expect that the asymptotic behavior would be determined by the smallest cross-section. In order to clarify this point, we consider an

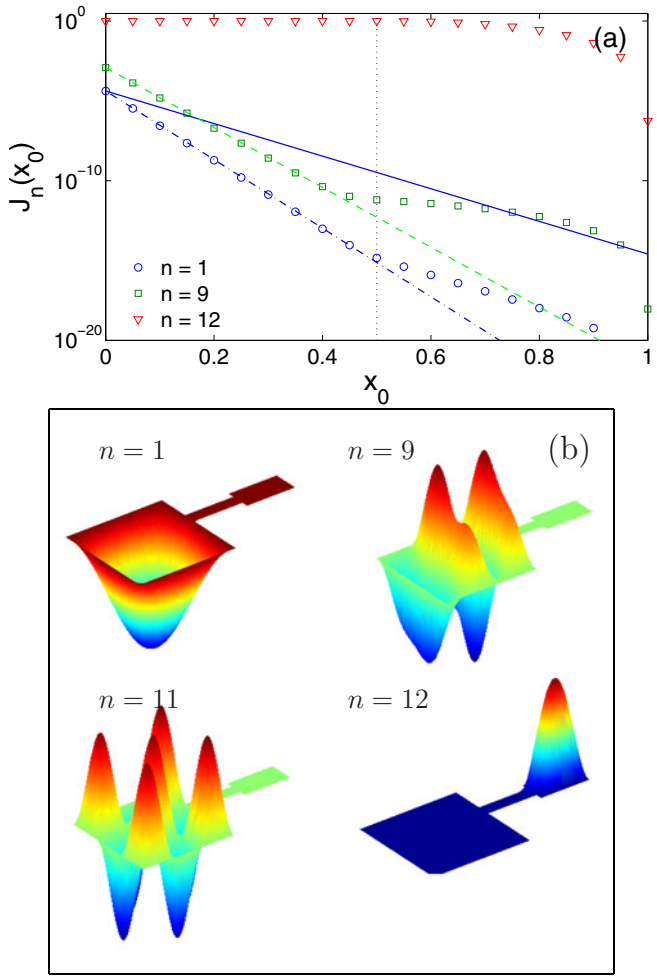

Fig. 5. (Color online) (a) The squared L_2-norm, $J_n(x_0)$, of three eigenfunctions with $n = 1, 9, 12$ (symbols) for the narrow-then-wide branch in Figure 2c. The upper bound (31) with $\mu = \pi^2/(1/4)^2$ is plotted for $n = 1$ by solid line. The hypothetical upper bound with $\mu = \pi^2/(1/8)^2$ is shown by dash-dotted ($n = 1$) and dashed ($n = 9$) lines. The vertical dotted line indicates the connection between two parts of the branch. (b) The corresponding eigenfunctions.

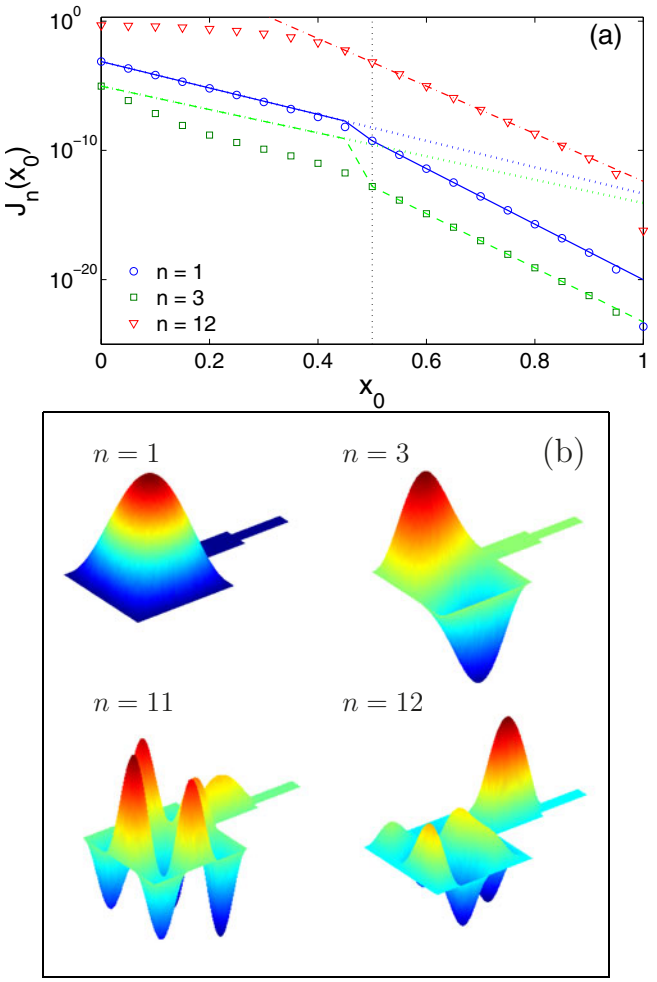

Fig. 6. (Color online) (a) The squared L_2-norm, $J_n(x_0)$, of three eigenfunctions with $n = 1, 3, 12$ (symbols) for the wide-then-narrow branch in Figure 2d. The upper bound (31) with $\mu = \pi^2/(1/4)^2$ is plotted by dotted lines for $n = 1$ and $n = 3$. The combined upper bound (for the wide part with $\mu = \pi^2/(1/4)^2$ and for the narrow part with $\mu = \pi^2/(1/8)^2$) is shown by solid ($n = 1$), dashed ($n = 3$) and dash-dotted ($n = 12$) lines. The vertical dotted line indicates the connection between two parts of the branch. (b) The corresponding eigenfunctions.

example in Figure 2c for which $\mu = \pi^2/(1/4)^2$. Although the narrow channel of width $b/2$ strongly attenuates the amplitude of the eigenfunction, it does not imply the exponential decay with a hypothetical rate $2\sqrt{4\mu - \lambda}$ along the next wider channel (Fig. 5). For instance, the function $J_1(x_0)$ exponentially decays with the rate $2\sqrt{4\mu - \lambda}$ (dashed line) up to $x_0 \approx 0.45$. However, this decay is slowed down for $x \geq 0.45$. The theoretical upper bound with the decay rate $2\sqrt{\mu - \lambda}$ (solid line) is of course applicable for all x_0 but it is not sharp.

If the wide channel is placed first (as shown in Fig. 2d), the situation is different. The decay rate $2\sqrt{\mu - \lambda}$, which is set by the largest cross-section length $b = 1/4$, can be used in the wide part of the branch. Although this result is also applicable in the narrow part, the upper bound here can be improved. In fact, if one considers the unit square and the wide branch as a basic domain, the decay rate for the narrow branch, $2\sqrt{4\mu - \lambda}$, is set by its width $b/2 = 1/8$ (Fig. 6). More generally, if the branch is a union of successive branches with progressively decreasing widths, one can combine the exponential upper bounds with progressively increasing decay rates.

Increasing branch

In the previous example in Figure 2c, the supplementary condition (15) was not satisfied on a part of the branch boundary. Nevertheless, the numerical computation confirmed the sharp decay rate (16). In order to check the relevance of the condition (15), we consider a linearly increasing branch shown in Figure 2e. Although the condition (15) is not satisfied at any point, the sharp decay

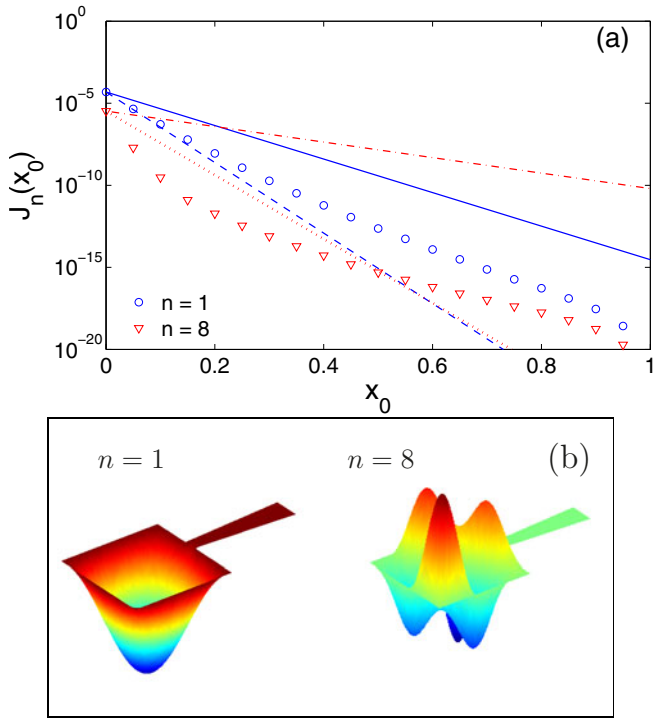

Fig. 7. (Color online) (a) The squared L_2-norm, $J_n(x_0)$, of two eigenfunctions with $n = 1, 8$ (symbols) for the increasing branch in Figure 2e. The upper bound (31) with $\mu = \pi^2/(1/4)^2$ is plotted by solid ($n = 1$) and dash-dotted ($n = 8$) lines. The hypothetical upper bound with $\mu = \pi^2/(1/8)^2$ is shown by dashed ($n = 1$) and dotted ($n = 8$) lines. (b) The corresponding eigenfunctions.

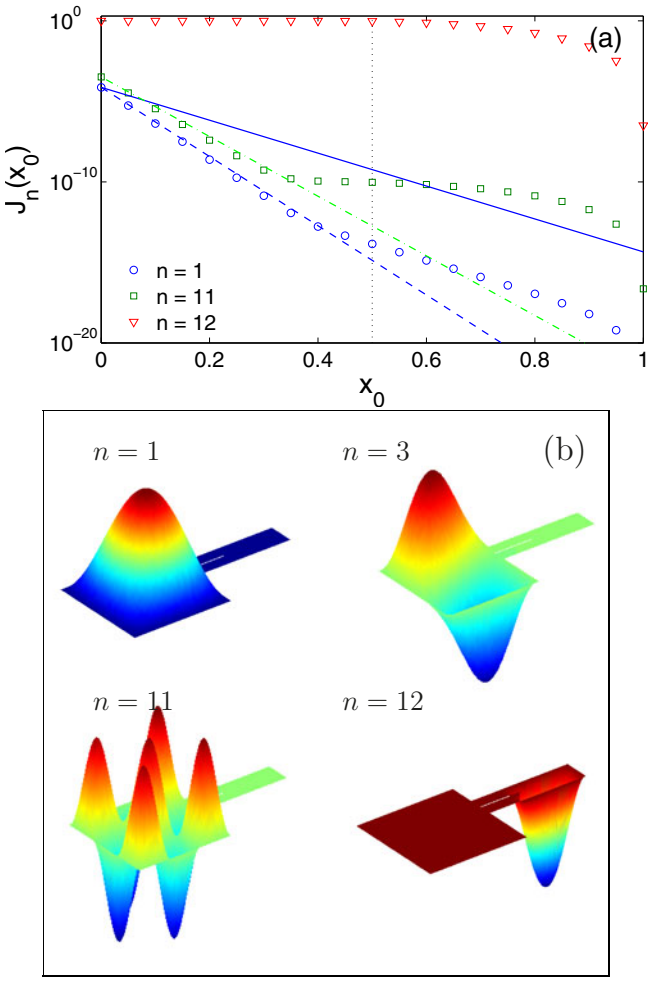

Fig. 8. (Color online) (a) The squared L_2-norm, $J_n(x_0)$, of three eigenfunctions with $n = 1, 11, 12$ (symbols) for the branch with a cut in Figure 2f. The upper bound (31) with $\mu = \pi^2/(1/4)^2$ is plotted by solid ($n = 1$) and dash-dotted ($n = 11$) lines. The hypothetical upper bound with $\mu = \pi^2/(1/8)^2$ for $n = 1$ is shown by dashed line. The vertical dotted line indicates the end of the cut. (b) The corresponding eigenfunctions.

rate (16) is again applicable, as shown in Figure 7. In a future work, one may try to relax the condition (15) or to provide counter-examples showing its relevance.

Branch with a cut

A small variation in the shape of the domain is known to result in small changes in eigenvalues of the Laplace operator, at least at the beginning of the spectrum (see Tab. 1). In turn, the eigenfunctions may be very sensitive to any perturbation of the domain. Bearing this sensitivity in mind, one can check the robustness of the exponential decay. We consider a horizontal cut at the middle of the rectangular branch (Fig. 2f). If the cut went along the whole branch, it would be equivalent to two separate rectangular branches of width $b/2$. In this case, the theoretical upper bound could be applied individually to each branch, and the value $\mu = \pi^2/(b/2)^2$ would be 4 times larger than for the original rectangular branch of width b. For a partial cut, whatever its length is, the theoretical decay rate is again determined by $\mu = \pi^2/(1/4)^2$ as for the rectangular branch. At the same time, it is clear that the cut results in a stronger "expelling" of eigenfunctions from the branch.

Figure 8a shows the squared L_2-norm, $J_n(x_0)$, of three eigenfunctions with $n = 1, 11, 12$. For the first eigenfunction, we plot two exponential upper bounds, one with the rigorous value $\mu = \pi^2/(1/4)^2$ and the other with a hypothetical value $\mu' = \pi^2/(1/8)^2 = 4\mu$ for a twice narrower branch (if the cut was complete). Although the first upper bound is of course applicable for the whole region, it is not sharp. In turn, the second upper bound is sharp but it works only up to $x_0 < 0.4$. One can see that for $x_0 > 0.4$, the slope of $\ln J_1(x_0)$ is given by the first decay rate. The best upper bound would be a combination of these two but its construction depends on the specific shape of the branch. It is worth noting that the transition between two upper bounds (i.e., the point x_0 around 0.4) does not appear at the end of the cut (here, at 0.5). This means that one cannot consider two subregions (with and without cut) separately in order to develop the individual upper bounds.

The 11th eigenvalue $\lambda_{11} \approx 177.0$ exceeds μ so that the rigorous decay rate is not applicable. In turn, the use of

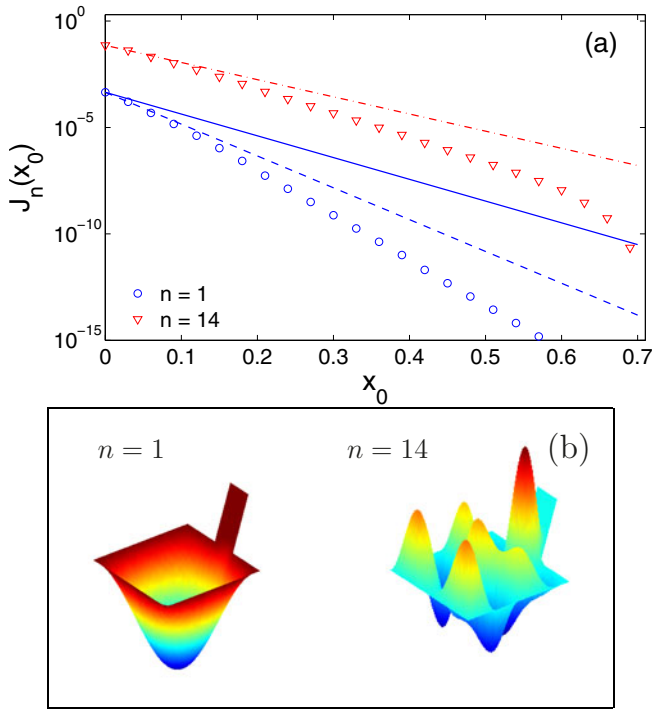

Fig. 9. (Color online) (a) The squared L_2-norm, $J_n(x_0)$, of two eigenfunctions with $n = 1, 14$ (symbols) for the tilted branch in Figure 2g. The formal upper bound (31) with $\mu = \pi^2/(1/4)^2$ is plotted by solid line for $n = 1$. The improved upper bound with $\mu = \pi^2/(1/4/\sqrt{2}))^2$ is shown by dashed ($n = 1$) and dash-dotted ($n = 14$) lines. (b) The corresponding eigenfunctions.

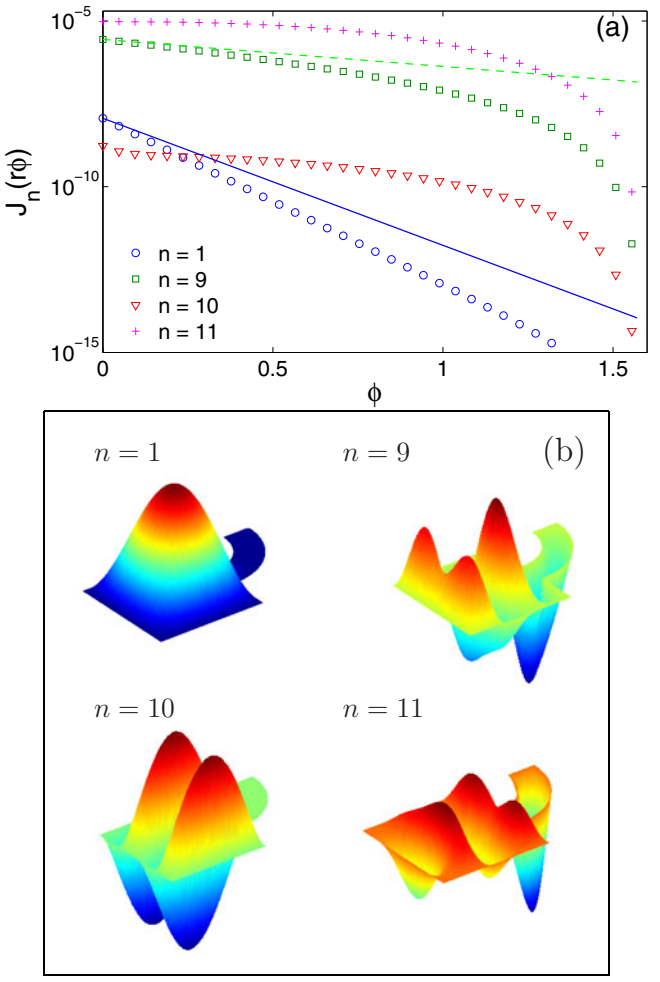

Fig. 10. (Color online) (a) The squared L_2-norm, $J_n(x_0')$, of four eigenfunctions with $n = 1, 9, 10, 11$ (symbols) for the circular branch in Figure 2h. The upper bound (31) with $\mu = \pi^2/(1/4)^2$ is plotted by solid ($n = 1$) and dashed ($n = 9$) lines. The curvilinear coordinate $x_0' = r\phi$ with $r = 3/8$ and the angle ϕ varying from 0 to $\pi/2$, was used. (b) The corresponding eigenfunctions.

the hypothetical value μ' provides a good upper bound up to $x_0 < 0.3$ but fails for $x_0 > 0.3$. Finally, the 12th eigenfunction has no exponential decay (in fact, it is localized in the branch).

Tilted and circular branches

Another interesting question concerns the parameterization of the branch Q. In Section 3, a variable shape of the branch was implemented through the cross-section profile $\Omega(x)$ where x ranged from 0 and a. The choice of the x coordinate is conventional and any other coordinate axis could be used instead of x (by rotating the domain). However, the freedom of rotation may lead to an inaccurate estimation of the decay rate. This point is illustrated by the domain in Figure 2g with a rectangular branch tilted by 45°. Applying formally the upper bound (13), one may expect the exponential decay with $\mu = \pi^2/(1/4)^2 \approx 157.91$. At the same time, if the whole domain was turned clockwise by 45° [or, equivalently, if the branch was parameterized along the axis x' in the direction $(1, 1)$], the decay rate would be set by $\mu = \pi^2/(1/4/\sqrt{2})^2 \approx 315.83$. It is clear that the behavior of eigenfunctions does not depend neither on rotations of the domain, nor on the parameterization of the branch. Figure 9 confirms the exponential decay with the latter threshold μ.

A circular branch in Figure 2h is another example, for which the choice of parameterization is important. Using the "conventional" parameterization by the x coordinate, the largest cross-section appears at $x = 3/8$, and it is equal to $1/2$ so that $\mu = \pi^2/(1/2)^2 \approx 39.48$. Only the first eigenvalue λ_1 is below μ so that the exponential upper bound is not formally applicable to other eigenfunctions. At the same time, it is clear that the circular branch of "true" width b can be naturally parameterized by the angle ϕ or, equivalently, by an arc, as illustrated in Figure 2h. However, there is an ambiguity in the choice between arcs of various radii (e.g., inner, outer or middle arcs). Although the length of all these arcs is proportional to the angle ϕ, the proportionality coefficient enters into the decay rate. For the results plotted in Figure 10, the inner arc of radius $r = 3/8$ was used. The squared L_2-norm was plotted as a function of the curvilinear coordinate $x_0' = r\phi$, with ϕ varying between 0 and $\pi/2$. For such a curvilinear parameterization, the width of the branch is constant, $b = 1/4$, so that there are 9 eigenvalues λ_n below $\mu = \pi^2/(1/4)^2$.

For instance, the exponential decay of the 9th eigenfunction is confirmed in Figure 10. For circular branches, rigorous upper bounds can be derived by writing explicit series representations of eigenfunctions in a circular annulus and reformulating the analysis similar to that of Section 2 (this analysis is beyond the scope of the paper). In general, an extension of the derivation in Section 3 to curvilinear parameterizations is an interesting perspective.

Branch with a small broadening

A small broadening in the middle of the branch is another interesting perturbation of the rectangular branch (Fig. 2i). Although this perturbation is small, the threshold value is reduced to $\mu = \pi^2/(1/2)^2 \approx 39.48$, instead of the value $\mu' = \pi^2/(1/4)^2 \approx 157.91$ for the rectangular branch. As a consequence, the sufficient condition $\lambda_n < \mu$ is satisfied only for $n = 1$, while for other n, the exponential upper bound (13) cannot be applied. One may thus wonder how do these eigenfunctions behave in the branch?

We checked that the 8 first eigenfunctions exponentially decay along the branch, similarly to the rectangular case. In turn, the 9th, 10th and some other eigenfunctions do not exhibit this behavior. Figure 11 illustrates this result for three eigenfunctions with $n = 1, 8, 9$. Since the rigorous upper bound is not applicable, we plot the function $J_n(0)\exp(-2\sqrt{\mu' - \lambda_n}x_0)$ with $\mu' = \pi^2/(1/4)^2$ as for the rectangular branch. One can see that this function correctly captures the behavior of $J_n(x_0)$ but fails to be its upper bound (there are regions in which $J_n(x_0)$ exceeds this function).

In summary, in spite of the fact that the condition $\lambda < \mu$ is not satisfied, the presence of a small broadening does not significantly affect the exponential decay of the first eigenfunctions but a hypothetical upper bound may not be valid.

Bifurcating branch

After describing the eigenfunctions in a single branch, one may wonder about their properties in a general pore network which consists of basic domains ("pores") connected by branches. In spite of numerous potential applications for diffusive transport in porous media, very little is known about this challenging problem. A dumbbell domain with a thin "handle" is probably the most studied case [24–27]. In particular, the method of matching asymptotic series yields the asymptotic estimates when the diameter of the channel is considered as a small parameter.

In order to illustrate the related difficulties, we consider a rectangular branch which bifurcates into two rectangular branches (Fig. 2j). For this example, the largest cross-section length is 1 so that $\mu = \pi^2 \approx 9.87$ and the exponential upper bound is not applicable. Figure 12 shows $J_n(x_0)$ for three eigenfunctions with $n = 1, 7, 8$ and the hypothetical upper bound with $\mu' = \pi^2/(1/4)^2$ as for the rectangular branch. The first eigenfunction is well bounded by the exponential function

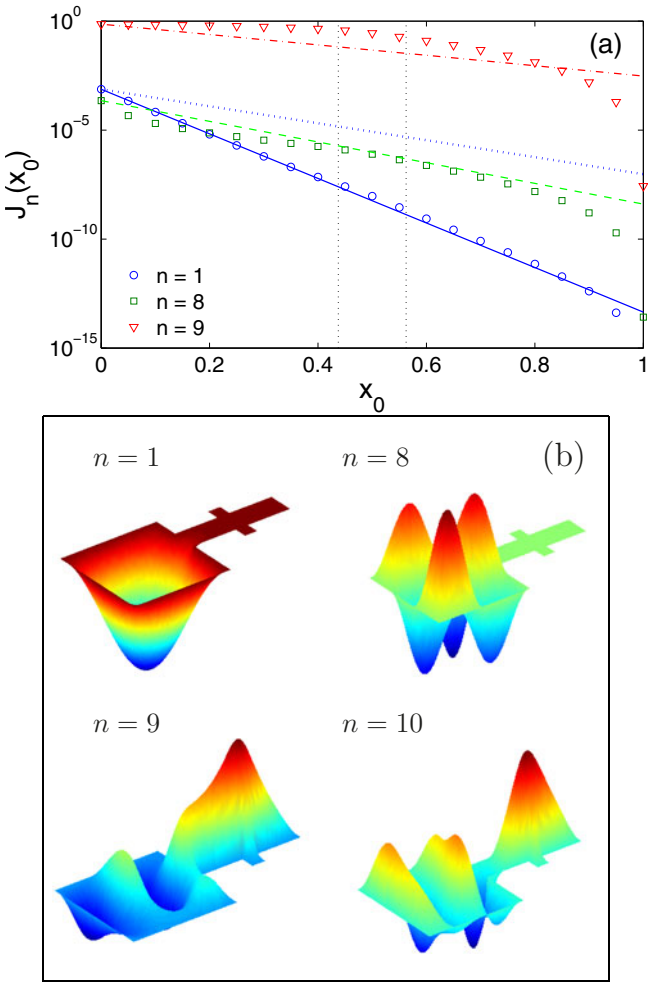

Fig. 11. (Color online) (a) The squared L_2-norm, $J_n(x_0)$, of three eigenfunctions with $n = 1, 8, 9$ (symbols) for the branch with a broadening in Figure 2i. The upper bound (31) with $\mu = \pi^2/(1/2)^2$ for $n = 1$ is shown by dotted line. The hypothetical upper bound (31) with $\mu = \pi^2/(1/4)^2$ is plotted by solid ($n = 1$), dashed ($n = 8$) and dash-dotted ($n = 9$) lines. Vertical dotted lines indicate the position of the broadening. (b) The corresponding eigenfunctions.

$J_1(0)\exp(-2\sqrt{\mu' - \lambda_1}x_0)$ for practically the whole length of the branch ($x_0 < 1$), with a small deviation at the bifurcation region ($x_0 > 1$). Similar behavior is observed for other eigenfunctions up to $n = 7$. The larger the index n, the earlier the deviation from the exponential upper bound appears (e.g., for $n = 7$, the upper bound works only for $x_0 < 0.3$). In turn, the 8th eigenfunction has no exponential decay in the branch as it is localized in the bifurcation region. At the same time, the corresponding eigenvalues are close: $\lambda_7 \approx 125.20$ and $\lambda_8 \approx 127.67$. This illustrates how significant may be the difference in properties of two consecutive eigenfunctions. We also emphasize on the difficulty of distinguishing these cases in general.

Surprisingly, an exponential decay can be recovered for thinner bifurcations of arbitrary length. Although this example may look specific, the arguments provided below are of general interest. In order to prove the exponential

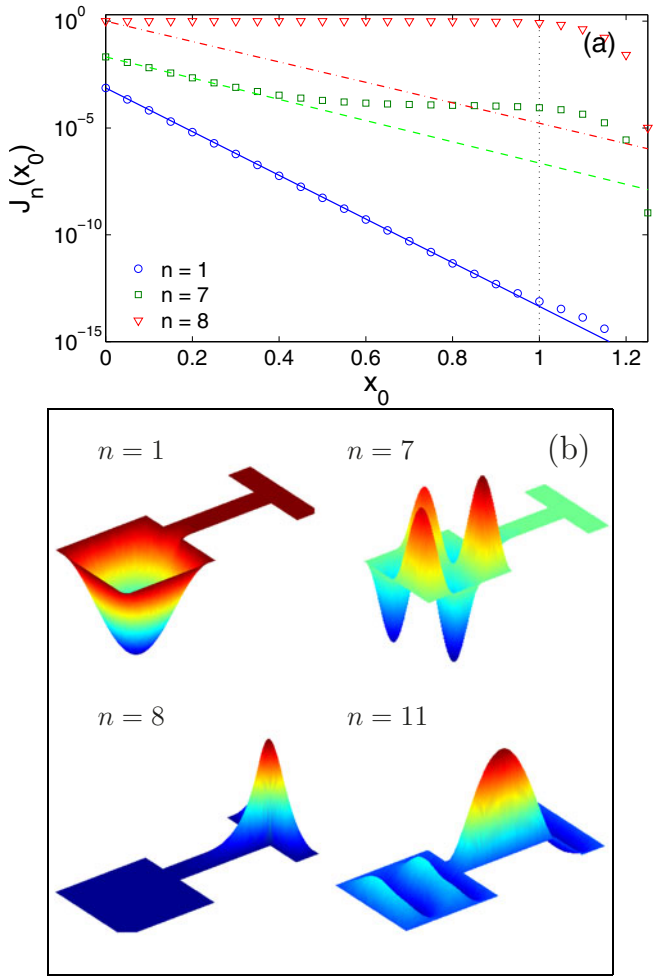

Fig. 12. (Color online) (a) The squared L_2-norm, $J_n(x_0)$, of three eigenfunctions with $n = 1, 7, 8$ (symbols) for the bifurcating branch in Figure 2j. The hypothetical upper bound (31) with $\mu = \pi^2/(1/4)^2$ is plotted by solid ($n = 1$), dashed ($n = 7$) and dash-dotted ($n = 8$) lines. The vertical dotted line indicates the position of bifurcation. (b) The corresponding eigenfunctions.

decay of the squared norm $J(x_0)$ in equation (29), we will establish the inequalities similar to those for $I(x_0)$ of Section 3. Replacing the norm $I(x_0)$ by the weaker norm $J(x_0)$ allows one to derive upper bounds in more general circumstances. Although we bear in mind the example shown in Figure 2j, the arguments are rather general and applicable in higher dimensions. By definition, one has

$$J'(x_0) = -I(x_0) = -\int\limits_{\Omega(x_0)} u^2(x_0, \mathbf{y})d\mathbf{y} < 0$$

and

$$J''(x_0) = -2\int\limits_{\Omega(x_0)} u\frac{\partial}{\partial x}ud\mathbf{y}$$
$$= 2\int\limits_{Q(x_0)} \big[(\nabla u, \nabla u) + u\Delta u\big]dxd\mathbf{y},$$

where the Green's formula, the identity $\partial/\partial x = -\partial/\partial n$ on $\Omega(x_0)$ and Dirichlet boundary condition on $\partial Q(x_0)\backslash\Omega(x_0)$ were used. The first integral can be bounded by splitting $Q(x_0)$ into two subdomains: $Q_1(x_0)$ (a part of the rectangular branch) and Q_2 (the bifurcation):

$$\int\limits_{Q(x_0)} (\nabla u, \nabla u)dxd\mathbf{y} \geq \mu \int\limits_{Q_1(x_0)} u^2dxd\mathbf{y} + \int\limits_{Q_2} (\nabla u, \nabla u)dxd\mathbf{y},$$

where the Friedrichs-Poincaré inequality was used with the smallest μ over $Q_1(x_0)$ (for the rectangular branch in Figure 2j, $\mu = \pi^2/b^2$). The separate analysis of two subdomains allowed us to exclude large cross-sections of the bifurcation Q_2 from the computation of μ.

In order to bound the second integral over Q_2, we note that

$$\nu_1 = \inf_{v\in H^1(Q_2),\ v|_\Gamma=0,\ v\neq 0} \frac{(\nabla v, \nabla v)}{(v, v)}$$

is the smallest eigenvalue of the Laplace operator in the rectangle Q_2 with Dirichlet boundary condition on the top, bottom and right segments (denoted by Γ) and Neumann boundary condition on the left segment. Since the eigenfunction u also belongs to $H^1(Q_2)$, one has

$$(\nabla u, \nabla u)_{L_2(Q_2)} \geq \nu_1(u, u)_{L_2(Q_2)},$$

from which

$$J''(x_0) \geq 2(\mu - \lambda)\int\limits_{Q_1(x_0)} u^2dxd\mathbf{y} + 2(\nu_1 - \lambda)\int\limits_{Q_2} u^2dxd\mathbf{y}.$$

If $\nu_1 > \mu$, we finally obtain

$$J''(x_0) \geq 2(\mu - \lambda)\int\limits_{Q(x_0)} u^2dxd\mathbf{y} = 2(\mu - \lambda)J(x_0).$$

As shown in Section 3, this inequality implies an exponential decay of $J(x_0)$.

If Q_2 is a rectangle of height h and width w with Dirichlet boundary condition on the top, bottom and right segments and Neumann boundary condition on the left segment, the smallest eigenvalue is $\nu_1 = \pi^2/h^2 + \pi^2/(2w)^2$. If the branch Q_1 is also a rectangle of width b (as shown in Fig. 2j), one has $\mu = \pi^2/b^2$. The condition $\nu_1 > \mu$ reads as $(b/h)^2 + (b/(2w))^2 > 1$. For instance, this condition is satisfied for any h if the bifurcation width w is smaller than $b/2$. In particular, this explains that a small broadening of width $b/2$ shown in Figure 2i does not degrade the exponential decay of $J_n(x_0)$ for $x_0 < 0.4375$. In turn, the bifurcation shown in Figure 2j with $h = 1$ and $w = b = 1/4$ does not fulfill the above condition as $(b/h)^2 + (b/(2w))^2 = 1/16 + 1/4 < 1$.

4.2 Infinite branches

In the derivation of Section 3, there was no condition on the length a of the branch. Even for an infinite branch, the

exponential decay is valid once the condition (11) is satisfied. However, when the branch is infinite, the Laplace operator eigenspectrum is not necessarily discrete so that L_2-normalized eigenfunctions may not exist. A simple counter-example is a semi-infinite strip $D = [0, \infty) \times [0, \pi]$ for which functions $\sinh(\sqrt{n^2 - \lambda}x)\sin(ny)$ satisfy the eigenvalue problem (8) but their $L_2(D)$ norms are infinite.

As shown by Rellich, if the first eigenvalue $\mu_1(x)$ in the cross-section $\Omega(x)$ of an infinite branch Q goes to infinity as $x \to \infty$, then there exist infinitely many L_2-normalized eigenfunctions [28]. In two dimensions, $\mu_1(x) = \pi^2/\ell(x)^2$ is related to the length $\ell(x)$ of the largest interval in the cross-section $\Omega(x)$. The condition $\mu_1(x) \to \infty$ requires thus $\ell(x) \to 0$. At the same time, the number of intervals in $\Omega(x)$ can increase with x so that the "total width" of the branch may arbitrarily increase.

For infinite decreasing branches, eigenfunctions can be shown to decay *faster* than an exponential with any decay rate. In fact, although the threshold μ was defined in (10) as the smallest $\mu_1(x)$ over all cross-sections of the branch, the separation into a basic domain and a branch was somewhat arbitrary. If the separation occurs at x_0 (instead of 0), one gets

$$I(x) \le I(x_0)\exp[-2\sqrt{\mu(x_0) - \lambda}\,(x - x_0)] \qquad (x \ge x_0),$$

where the new threshold $\mu(x_0) = \inf_{x_0 < x} \mu_1(x)$ increases with x_0, while the prefactor $I(x_0)$ also decays exponentially with x_0 according to equation (13). Since the above upper bound is applicable for any x_0, one can take x_0 to be a slowly increasing function of x [its choice depends on $\mu(x_0)$] that would result in a faster-than-exponential decay of $I(x)$. This result is a consequence of the condition $\mu_1(x) \to \infty$ as x goes to infinity.

4.3 Three-dimensional domains

The exponential upper bound (13) becomes still more interesting in three (and higher) dimensions. While any cross-section $\Omega(x)$ was a union of intervals in two dimensions, the shape of cross-sections in three dimensions can vary significantly (e.g., see Fig. 1c). Whatever the shape of the branch is, the only relevant information for the exponential decay is the smallest eigenvalue μ in all cross-sections $\Omega(x)$. For instance, for a variable rectangular profile of the branch, $\Omega(x) = [0, b(x)] \times [0, c(x)]$, the first eigenvalue $\mu_1(x) = \frac{\pi^2}{b(x)^2} + \frac{\pi^2}{c(x)^2}$ can remain bounded from below by some μ even if one of the sides $b(x)$ or $c(x)$ grows to infinity. This means that eigenfunctions may exponentially decay even in infinitely growing branches.

4.4 Neumann boundary condition

The theoretical derivation in Section 3 essentially relies on the Dirichlet boundary condition on the branch boundary: $u|_{\partial Q} = 0$. This condition can be interpreted, e.g., as a rigid fixation of a vibrating membrane at the boundary, or as a perfect absorption of diffusing particles at the boundary. The opposite case of free vibrations of the membrane or a perfect reflection of particles is described by Neumann boundary condition, $\partial u/\partial n|_{\partial Q} = 0$. Although the eigenvalue problem may look similar, the behavior of eigenfunctions is different. In particular, an extension of the results of Section 3 fails even in the simplest case of a rectangular branch, as illustrated in Figure 13. Although the 8 first eigenvalues λ_n are below $\mu = \pi^2/(1/4)^2$, only some of them decay exponentially (e.g., with $n = 4$). This decay is related to the reflection symmetry of the domain. In fact, the eigenfunctions with $n = 4, 10$ are anti-symmetric so that they are 0 along the horizontal symmetry line. One can therefore split the domain into two symmetric subdomains and impose the Dirichlet boundary condition on the splitting line (Figs. 2a and 2b). For this mixed Dirichlet-Neumann boundary condition, the exponential decay of eigenfunctions can be derived in a weaker form (see Appendix C).

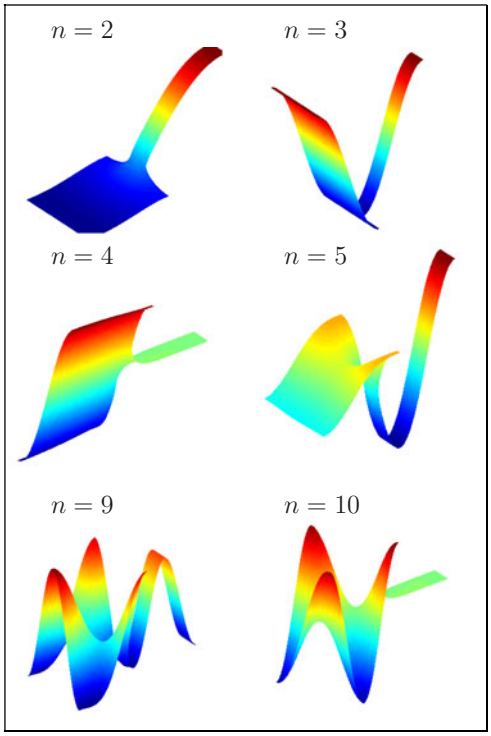

Fig. 13. (Color online) Six eigenfunctions with $n = 2$, 3, 4, 5, 9, 10 for the rectangular branch (Fig. 2a) with Neumann boundary condition (the fundamental eigenfunction with $n = 1$ is constant and not shown).

4.5 Expelling from the branch

It is important to stress that the "smallness" of an eigenfunction in the branch and its exponential decay are different notions which should not be confused. In fact, an eigenfunction can be small in the branch either due to a rapid exponential decay, or because of the small constant $I_n(0)$ or $J_n(0)$ in front of the exponential function.

For instance, Figure 10a shows the behavior of $J_{10}(x_0)$ without an exponential decay, but the eigenfunction is nevertheless small (Fig. 10b). Another example in Figure 4a with $n = 9$ illustrates the opposite situation: the eigenfunction decays exponentially along the branch but it does not look small.

Conclusion

We have studied the behavior of the Laplace operator eigenfunctions in a large class of domains composed of a basic domain of arbitrary shape and a branch Q which can be parameterized by a variable cross-sectional profile $\Omega(x)$. We have rigorously proved that each eigenfunction whose eigenvalue λ is smaller than the threshold $\mu = \inf\{\mu_1(x)\}$, exponentially decays inside the branch, where $\mu_1(x)$ is the first eigenvalue of the Laplace operator in the cross-section $\Omega(x)$. In general, the decay rate was shown to be at least $\sqrt{2}\sqrt{\mu-\lambda}$. For non-increasing branches, the decay rate $2\sqrt{\mu-\lambda}$ was derived and shown to be sharp for an appropriate parameterization of the branch. The exponential upper bound is applicable in any dimension and for finite and infinite branches. In the latter case, the condition $\mu_1(x) \to \infty$ as $x \to \infty$ is imposed to ensure the existence of L_2-normalized eigenfunctions. Since the derivation did not involve any information about the basic domain V, the exponential upper bound is applicable for arbitrary V with any boundary condition on ∂V for which the Laplace operator in D is still self-adjoint. In turn, the Dirichlet boundary condition on the branch boundary was essential (although a weaker exponentially decaying upper bound were also derived for anti-symmetric eigenfunctions with Neumann boundary condition, see Appendix C).

The numerical solutions of the eigenvalue problem have been used to illustrate and extend the theoretical results. It was shown that the sufficient condition $\lambda < \mu$ is not necessary, i.e., the eigenfunctions may exponentially decay even if $\lambda > \mu$. However, in this case, the decay rate and the range of its applicability strongly depend on the specific shape of the branch. For all numerical examples, the sharp decay rate $2\sqrt{\mu-\lambda}$ was correct, even when the condition (15) of non-increasing branches was not satisfied. In future, it would be interesting either to relax this condition, or to find counter-examples, for which the sharp decay is not applicable.

Our results significantly extend the classical exponential upper bounds for branches of a *constant* cross-section [15]. A rigorous upper bound for different norms of Laplacian eigenfunctions in branches of *variable* cross-sectional profile is also a new achievement in the theory of classical and quantum waveguides, with potential applications in microelectronics, optics and acoustics. The mathematical methods of the paper can be adapted for studying eigenfunctions for various spectral problems or other types of domains.

This work has been partly supported by the RFBR N 09-01-00408a grant and the ANR grant "SAMOVAR".

Appendix A: Derivation for rectangular branch

From the inequality $\sinh x \le \cosh x$, equation (5) is bounded as

$$||\nabla u||^2_{L_2(Q(x_0))} \le \frac{b}{2}\sum_{n=1}^{\infty} c_n^2 \left[\left(\frac{\pi}{b}n\right)^2 + \gamma_n^2\right] \times \int_{x_0}^{a} \cosh^2\left(\gamma_n(a-x)\right) dx.$$

The last integral is bounded as

$$\int_{x_0}^{a} \cosh^2\left(\gamma_n(a-x)\right) dx \le \int_{x_0}^{a} e^{2\gamma_n(a-x)} dx = \frac{e^{2\gamma_n a}}{2\gamma_n} \times \left(e^{-2\gamma_n x_0} - e^{-2\gamma_n a}\right) \le \frac{e^{2\gamma_n a}}{2\gamma_n} e^{-2\gamma_n x_0} \le \frac{e^{2\gamma_n a}}{2\gamma_n} e^{-2\gamma_1 x_0},$$

where we used the inequality $\cosh x \le e^x$ for $x \ge 0$ and the fact that $\gamma_n = \sqrt{\pi^2 n^2/b^2 - \lambda}$ increases with n. We have then

$$||\nabla u||^2_{L_2(Q(x_0))} \le \frac{b}{2} e^{-2\gamma_1 x_0} \sum_{n=1}^{\infty} c_n^2 \left[\frac{\pi^2}{b^2}\frac{n^2}{2\gamma_n} + \frac{\gamma_n}{2}\right] e^{2\gamma_n a}.$$

Writing two inequalities:

$$\gamma_n = \sqrt{\pi^2 n^2/b^2 - \lambda} \le \frac{\pi}{b} n,$$

$$\frac{n^2}{\gamma_n} = \frac{n}{(\pi/b)\sqrt{1 - \lambda b^2/(\pi^2 n^2)}} \le C_1 n,$$

where C_1 is a constant, one gets an upper bound in the order of n for the expression in large brackets. Finally, we have a bound for $e^{2\gamma_n a}$ as

$$\sinh^2(2\gamma_n a) = \frac{e^{2\gamma_n a}}{4}\left(1 - e^{-2\gamma_n a}\right)^2 \ge \frac{e^{2\gamma_n a}}{4}\left(1 - e^{-2\gamma_1 a}\right)^2,$$

from which

$$e^{2\gamma_n a} \le C_2 \sinh^2(2\gamma_n a),$$

with a constant $C_2 = 4/(1 - e^{-2\gamma_1 a})^2$. Bringing together these inequalities, we get the bound (6).

A.1 Trace theorem

The trace theorem implies [29] that the series

$$f(x) \equiv \sum_{n=1}^{\infty} n \left(u(x,y), \sin(\pi n y/b)\right)^2_{L_2(0,b)},$$

which is equivalent to the squared norm of $u(x,y)$ in the Sobolev space $H^{1/2}_{(0,b)}$, may be bounded from above by the

norm $||\nabla u||^2_{L_2(D)}$. For completeness, we provide the proof for our special case. For a fixed x, we denote

$$X_n(x) \equiv \big(u(x,y), \sin(\pi n y/b)\big)_{L_2(0,b)}$$

the Fourier coefficients of the function $u(x,y)$:

$$u(x,y) = \frac{2}{b}\sum_{n=1}^{\infty} X_n(x)\sin(\pi n y/b).$$

On one hand, starting from $X_n(a) = 0$, one gets

$$X_n^2(x) = \left|\int_x^a (X_n^2)' dx_1\right| = 2\left|\int_x^a X_n X_n' dx_1\right|,$$

while the Cauchy inequality implies

$$2\left|\int_x^a X_n X_n' dx_1\right| \le 2||X_n||_{L_2(0,a)}||X_n'||_{L_2(0,a)}.$$

The inequality $2\alpha\beta \le \alpha^2 + \beta^2$ yields

$$2(\pi n/b)||X_n||_{L_2(0,a)}||X_n'||_{L_2(0,a)} \le ||X_n'||^2_{L_2(0,a)} + (\pi n/b)^2||X_n||^2_{L_2(0,a)},$$

from which

$$(\pi n/b)X_n^2(x) \le ||X_n'||^2_{L_2(0,a)} + (\pi n/b)^2||X_n||^2_{L_2(0,a)}.$$

On the other hand, we write explicitly the energetic norm of u:

$$||\nabla u||^2_{L_2(Q)} = \frac{2}{b}\sum_{n=1}^{\infty}\Big(||X_n'||^2_{L_2(0,a)} + (\pi n/b)^2||X_n||^2_{L_2(0,a)}\Big),$$

from which

$$f(x) = \sum_{n=1}^{\infty} nX_n^2(x) \le \frac{b^2}{2\pi}||\nabla u||^2_{L_2(Q)} \le \frac{b^2}{2\pi}||\nabla u||^2_{L_2(D)}.$$

Since the coefficients $X_n(x)$ and c_n are related as

$$X_n(x) = \frac{b}{2}\, c_n \sinh(\gamma_n(a-x)),$$

the substitution of $x = 0$ into this equation yields

$$\sum_{n=1}^{\infty} nc_n^2 \sinh^2(\gamma_n a) = \frac{4}{b^2}\sum_{n=1}^{\infty} nX_n(0)^2 = \frac{4}{b^2}f(0) \le \frac{2\lambda}{\pi}||u||^2_{L_2(D)} = \frac{2\lambda}{\pi}||u||^2_{L_2(D)}.$$

Appendix B: Several classical results

For completeness, we recall the derivation of several classical results [29,30] which are well known for spectral analysts but may be unfamiliar for other readers.

B.1 Rayleigh's principle

Let us start with the first eigenvalue λ_1 of the problem (1) which can be found as

$$\lambda_1 = \inf_{v\in \overset{\circ}{H}{}^1} \frac{(\nabla v, \nabla v)_{L_2(D)}}{(v,v)_{L_2(D)}}, \tag{B.1}$$

where $\overset{\circ}{H}{}^1 = \{v \in L_2(D),\ \partial v/\partial x_i \in L_2(D),\ i = 1, \ldots, n+1,\ v|_{\partial D} = 0\}$. Denoting ϕ_1 the first eigenfunction in equation (28), one takes

$$v = \begin{cases} \phi_1, & (x,\mathbf{y}) \in V, \\ 0, & (x,\mathbf{y}) \notin V, \end{cases}$$

as a trial function in equation (B.1) to obtain

$$\lambda_1 < \frac{(\nabla\phi_1, \nabla\phi_1)_{L_2(V)}}{(\phi_1,\phi_1)_{L_2(V)}} = \kappa_1,$$

i.e., the first eigenvalue λ_1 in the whole domain D is always smaller than the first eigenvalue κ_1 in its subdomain V. More generally, if there are n eigenvalues $\kappa_1 \le \ldots \le \kappa_n \le \mu$ then there exist n eigenvalues $\lambda_1 \le \ldots \le \lambda_n < \mu$.

Note that the Friedrichs-Poincaré inequality (21) follows from equation (B.1).

B.2 Rellich's identity

Let u be an eigenfunction which satisfies the equation

$$\Delta u + \lambda u = 0, \quad (x,\mathbf{y}) \in D, \quad u|_{\partial D} = 0.$$

We multiply this equation by $\frac{\partial u}{\partial x}$ and integrate over the domain $Q(x_0)$ defined by equation (23):

$$\int_{Q(x_0)} \frac{\partial u}{dx}\Delta u\, dxd\mathbf{y} + \lambda \int_{Q(x_0)} u\frac{\partial u}{dx}\, dxd\mathbf{y} = 0. \tag{B.2}$$

The second integral can be transformed as

$$\begin{aligned}\lambda \int_{Q(x_0)} u\frac{\partial u}{dx}\, dxd\mathbf{y} &= \frac{\lambda}{2}\int_{Q(x_0)}\left(\frac{\partial}{\partial x}u^2\right)dxd\mathbf{y} \\ &= -\frac{\lambda}{2}\int_{\partial Q(x_0)} u^2(x_0,\mathbf{y})(\mathbf{e}_x,\mathbf{n})dS \\ &= -\frac{\lambda}{2}\int_{\Omega(x_0)} u^2(x_0,\mathbf{y})d\mathbf{y},\end{aligned} \tag{B.3}$$

where $\mathbf{n} = \mathbf{n}(S)$ is the unit normal vector at $S \in \partial Q(x_0)$ and the boundary condition $u_{|\partial D} = 0$ was used on $\Gamma(x_0) = \partial Q(x_0)\backslash\Omega(x_0)$.

Using the Green's formula, the first integral in equation (B.2) can be transformed to

$$\int_{Q(x_0)} \frac{\partial u}{\partial x}\Delta u dxd\mathbf{y} = \int_{\partial Q(x_0)} \frac{\partial u}{\partial x}\frac{\partial u}{\partial n}dS - \int_{Q(x_0)}\left(\nabla u, \nabla\frac{\partial u}{\partial x}\right)dxd\mathbf{y}. \tag{B.4}$$

The first integral over $\partial Q(x_0)$ can be split in two terms:

$$\int\limits_{\partial Q(x_0)} \frac{\partial u}{\partial x}\frac{\partial u}{\partial n}dS = \int\limits_{\Gamma(x_0)} \frac{\partial u}{\partial x}\frac{\partial u}{\partial n}dS - \int\limits_{\Omega(x_0)} \left(\frac{\partial u}{\partial x}\right)^2 d\mathbf{y},$$

where $\partial/\partial n = (\mathbf{n}, \nabla)$ is the normal derivative pointing outwards the domain, and the sign minus appears because $\partial u/\partial n = -\partial u/\partial x$ at $\Omega(x_0)$.

The second integral in equation (B.4) is

$$\int\limits_{Q(x_0)} \left(\nabla u, \nabla \frac{\partial u}{\partial x}\right) dxd\mathbf{y} = \frac{1}{2}\int\limits_{Q(x_0)} \frac{\partial}{\partial x}(\nabla u, \nabla u) dxd\mathbf{y}$$
$$= \frac{1}{2}\int\limits_{\Gamma(x_0)} (\nabla u, \nabla u)(\mathbf{e}_x, \mathbf{n}) dS + \frac{1}{2}\int\limits_{\Omega(x_0)} (\nabla u, \nabla u) d\mathbf{y}.$$

Taking into account the Dirichlet boundary condition $u|_{\Gamma(x_0)} = 0$, one has

$$(\nabla u)|_{\Gamma(x_0)} = \mathbf{n}\frac{\partial u}{\partial n}|_{\Gamma(x_0)},$$
$$\frac{\partial u}{\partial x}|_{\Gamma(x_0)} = (\mathbf{e}_x, \nabla u) = (\mathbf{e}_x, \mathbf{n})\frac{\partial u}{\partial n}|_{\Gamma(x_0)}.$$

Combining these relations, one gets

$$\int\limits_{Q(x_0)} \frac{\partial u}{\partial x}\Delta u \; dxd\mathbf{y} = \frac{1}{2}\int\limits_{\Gamma(x_0)} \left(\frac{\partial u}{\partial n}\right)^2 (\mathbf{e}_x, \mathbf{n}) dS$$
$$-\frac{1}{2}\int\limits_{\Omega(x_0)} \left(\frac{\partial u}{\partial x}\right)^2 d\mathbf{y} + \frac{1}{2}\int\limits_{\Omega(x_0)} (\nabla_\perp u, \nabla_\perp u) d\mathbf{y},$$

from which and equations (B.2), (B.3) the Rellich's identity (22) follows.

Appendix C: Derivation for Neumann boundary condition

We consider the eigenvalue problem for the Laplace operator with Neumann boundary condition:

$$-\Delta u(x, \mathbf{y}) = \lambda u(x, \mathbf{y}), \quad (x, \mathbf{y}) \in D, \qquad (\partial u/\partial n)_{|\partial D} = 0.$$

In general, these eigenfunctions may not exponentially decay along a branch, with a trivial counter-example being the first eigenfunction u_1 which is constant over the whole domain D (and $\lambda_1 = 0$).

If a domain D is symmetric with respect to a hyperplane Γ, there exist eigenfunctions which are anti-symmetric with respect to Γ and thus 0 at Γ. In order to study such anti-symmetric eigenfunctions, one can consider the "half-domain" with mixed Dirichlet-Neumann boundary condition and prove the exponential decay in a weaker form than the results of Section 3. For simplicity, we assume that the branch Q is defined as $Q = \{(x, \mathbf{y}) \in \mathbb{R}^{n+1}\colon\ 0 \le x < a,\ |\mathbf{y}| < f(x)\}$, with a piecewise smooth non-negative function $f(x)$. Each cross-section $\Omega(x)$ is an n-dimensional ball of radius $f(x)$. Moreover, we impose two supplementary conditions: $f'(x) \le 0$ (i.e., the branch is not increasing) and $f(a) = 0$. If the eigenvalue λ is smaller than the smallest eigenvalue μ over the cross-sections $\Omega(x)$ of Q, then the associated eigenfunction u decays exponentially along the branch. Denoting

$$J(x_0) \equiv \frac{1}{w_n}\int\limits_{Q(x_0)} |u(x, \mathbf{y})|^2 dxd\mathbf{y},$$

where $Q(x_0) = \{(x, \mathbf{y}) \in \mathbb{R}^{n+1}\colon\ x_0 \le x < a,\ |\mathbf{y}| < f(x)\} \subset Q$ and w_n is the volume of the unit n-dimensional ball, we derive

$$J(x_0) \le J(0)\exp\left(-\sqrt{2}\sqrt{\mu - \lambda}\; x_0\right), \quad (0 \le x_0 < a). \tag{C.5}$$

It is worth stressing that this inequality is weaker that (13) because the L_2-norm over the cross-section $\Omega(x_0)$ is replaced by the L_2-norm over the subdomain $Q(x_0)$. The prefactor $1/w_n$ was introduced for convenience.

As in Section 3, the proof relies on the Maslov's inequality (17). We have

$$J(x_0) = \int\limits_{x_0}^{a} dx \int\limits_0^{f(x)} r^{n-1}u^2(x, r)dr,$$
$$J'(x_0) = -\int\limits_0^{f(x_0)} r^{n-1}u^2(x_0, r)dr,$$
$$J''(x_0) = -2\int\limits_0^{f(x_0)} r^{n-1}u(x_0, r)dr\frac{\partial u}{\partial x}$$
$$-u^2(x_0, f(x_0))[f(x_0)]^{n-1}f'(x_0). \tag{C.6}$$

For the first term in the last equality, one uses the Green's formula to get

$$\int\limits_{Q(x_0)} u\Delta u dxd\mathbf{y} + \int\limits_{Q(x_0)} |\nabla u|^2 dxd\mathbf{y} = \int\limits_{\partial Q(x_0)} u\frac{\partial u}{\partial n}dS$$
$$= -w_n\int\limits_0^{f(x_0)} r^{n-1}\; u(x_0, r)\frac{\partial u}{\partial x}dr,$$

because the integral over other parts of the boundary $\partial Q(x_0)$ vanishes, and $\partial u/\partial n = -\partial u/\partial x$ over the cross-section $\Omega(x_0)$. Using the Friedrichs-Poincaré inequality, one finally gets

$$J''(x_0) = \frac{2}{w_n}\int\limits_{Q(x_0)} \left(|\nabla u|^2 + u\Delta u\right) dxd\mathbf{y}$$
$$- u^2(x_0, f(x_0))f'(x_0)$$
$$\ge \frac{2(\mu - \lambda)}{w_n}\int\limits_{Q(x_0)} u^2(x, \mathbf{y})dxd\mathbf{y} = 2(\mu - \lambda)J(x_0),$$

where the condition $f'(x) \leq 0$ was used to omit the last term. The Maslov's inequality is established.

In order to apply this inequality, we also need to get the following relations

$$J(a) = 0, \quad J'(a) = 0, \quad J(x_0) \neq 0, \quad J'(x_0) < 0.$$

The first two relations are ensured by the condition $f(a) = 0$, while the last relation follows directly from (C.6). The third inequality holds due to the conditions $f'(x) \leq 0$ and $f(a) = 0$.

Finally, the exponentially decaying upper bound (C.5) for $J(x_0)$ can be obtained in the same way as in Section 3.

References

1. R. Courant, D. Hilbert, *Methods of Mathematical Physics* (Wiley, New York, 1989), Vol. 1, p. 302
2. B. Sapoval, T. Gobron, A. Margolina, Phys. Rev. Lett. **67**, 2974 (1991).
3. B. Sapoval, T. Gobron, Phys. Rev. E **47**, 3013 (1993)
4. S. Russ, B. Sapoval, O. Haeberlé, Phys. Rev. E **55**, 1413 (1997)
5. B. Sapoval, O. Haeberlé, S. Russ, J. Acoust. Soc. Am. **102**, 2014 (1997)
6. O. Haeberlé, B. Sapoval, K. Menou, H. Vach, Appl. Phys. Lett. **73**, 3357 (1998)
7. B. Hébert, B. Sapoval, S. Russ, J. Acoust. Soc. Am. **105**, 1567 (1999)
8. C. Even, S. Russ, V. Repain, P. Pieranski, B. Sapoval, Phys. Rev. Lett. **83**, 726 (1999)
9. S. Russ, B. Sapoval, Phys. Rev. E **65**, 036614 (2002)
10. S. Felix, M. Asch, M. Filoche, B. Sapoval, J. Sound. Vibr. **299**, 965 (2007)
11. M. Filoche, S. Mayboroda, Phys. Rev. Lett. **103**, 254301 (2009)
12. S.M. Heilman, R.S. Strichartz, Notices Amer. Math. Soc. **57**, 624 (2010)
13. B. Daudert, M. Lapidus, Fractals **15**, 255 (2007)
14. A.L. Delitsyn, B.-T. Nguyen, D.S. Grebenkov, Eur. Phys. J. B **85**, 176 (2012)
15. J.D. Jackson, *Classical Electrodynamics*, 3rd edn. (Wiley & Sons, New York, 1999).
16. J. Goldstone, R.L. Jaffe, Phys. Rev. B **45**, 14100 (1992)
17. J.P. Carini, J.T. Londergan, K. Mullen, D.P. Murdock, Phys. Rev. B **48**, 4503 (1993)
18. E.E. Schnol', Mat. Sb. **42**, 273 (1957)
19. Y.B. Orocko, Math. USSR Sb. **22**, 167 (1974)
20. S. Agmon, *Lectures on Exponential Decay of Solution of Second-Order Elliptic Equation* (Princton Univercity Press, 1982).
21. V.P. Maslov, Sov. Math. Surv. **19**, 199 (1964) [in Russian]
22. V.P. Maslov, *Perturbation Theory and Asymptotic Methods* (Moscow State University, Moscow, 1965) [in Russian]
23. P. Grisvard, *Elliptic Problem for Nonsmooth Domain* (Pitman Advanced Publishing Company, Boston, 1985).
24. J.T. Beale, Commun. Pure Appl. Math. **26**, 549 (1973)
25. R.R. Gadyl'shin, Math. Notes **54**, 1192 (1993)
26. R.R. Gadyl'shin, Math. Notes **55**, 14 (1994)
27. R.R. Gadyl'shin, Izv. Math. **69**, 265 (2005)
28. F. Rellich, *Das Eigenwertproblem von in Halbrohren* (Studies and essays presented to R. Courant, New York, 1948), pp. 329–344
29. J.L. Lions, E. Magenes, *Non-homogeneous Boundary Value Problems and Applications* (Springer-Verlag, 1972)
30. I.M. Glazman, *Direct Methods of Qualitative Spectral Analysis of Singular Differential Operators* (Fizmathgiz, Moscow, 1963; Translated in English in 1965)